Dynamic Meteorology-Induced Emissions Coupler (MetEmis) development in the Community Multiscale Air Quality (CMAQ): CMAQ-MetEmis

Bok H. Baek[1], Carlie Coats[1], Siqi Ma[1,2], Chi-Tsan Wang[1], Yunyao Li[1], Jia Xing[1], Daniel Tong[1,2], Soontae Kim[4], and Jung-Hun Woo[3*]

[1]Center for Spatial Information Science and Systems, George Mason University, Fairfax, VA 22030, USA
[2] Department of Atmospheric, Oceanic and Earth Sciences, George Mason University, Fairfax, VA 22030, USA
[3] Civil and Environmental Engineering, College of Engineering, Konkuk University, Seoul, Republic of Korea
[4] Environmental Engineering, College of Engineering, Ajou University, Suwon, Republic of Korea

Correspondence to: Jung-Hun Woo (jwoo@konkuk.ac.kr)

Abstract

There have been consistent efforts to improve the spatiotemporal representations of biogenic/anthropogenic emission sources for photochemical transport modeling for better accuracy of local/regional air quality forecasts. While biogenic emissions, bi-directional NH_3 from fertilizer applications, and point-source plume rise are dynamically coupled in CMAQ "*inline*", there are still known meteorology-induced emissions sectors (e.g., onroad mobile, residential heating, and livestock wastes) with little or no accounting of meteorological impacts in current operational chemical and aerosol forecasts but are represented with static, no-weather-aware annual or monthly county total emissions and standard monthly/weekly/daily temporal allocation profiles to disaggregate them on finer time scales for the hourly air quality forecasts. It often results in poor forecasting performance due to the poor spatiotemporal representations of precursor pollutants during high ozone and $PM_{2.5}$ episodes. The main focus of this study is to develop a dynamic "*inline*" coupler within CMAQ system for the onroad mobile emission sector that requires significant computational resources in current modeling application. To improve their accuracy and spatiotemporal representations, we developed the "*inline*" coupler module called "CMAQ-MetEmis" for Meteorology-Induced Emission sources within the Community Multiscale Air Quality (CMAQ) version 5.3.2 modeling system. It can dynamically estimate meteorology-induced hourly gridded onroad mobile emissions within the CMAQ using simulated meteorology without any computational burden to the CMAQ modeling system.

To understand the impacts of meteorology-driven onroad mobile emissions on local air quality, the CMAQ is applied over the continental U.S. for two months (January and July 2019) for two emissions scenarios: a) "*static*" onroad vehicle emissions based on static temporal profiles, and b) "*inline*" CMAQ-MetEmis onroad vehicle emissions. Overall, the "CMAQ-MetEmis" coupler allows us to dynamically simulate onroad vehicle emissions from the MOVES onroad emission model for CMAQ with a better spatiotemporal representation based on the simulated meteorology inputs, compared to the "*static*" scenario. The domain total of daily VOC emissions from the "*inline*" scenario shows the largest impacts from the local meteorology, which is approximately 10% lower than the ones from the "*static*" scenario. Especially, the major difference of VOC estimates was shown over the California region. These local meteorology impacts on onroad vehicle emissions via CMAQ-MetEmis revealed an improvement in hourly NO_2, daily maximum ozone, and daily average $PM_{2.5}$ patterns with a higher agreement and correlation with daily ground observations.

Keywords: CMAQ, CTM, weather-aware emissions, vehicle emissions, inline modeling

1. Introduction

Since the industrial revolution, the chemical pollutants in the atmosphere have impacted human society due to their adverse health effects. The primary gases and particles directly emitted from their emission sources are chemically transformed into secondary pollutants through complex chemical reactions under various local meteorological conditions. Over last three decades, sophisticated multiscale chemical transport models (CTM) have been developed to predict the concentrations of primary and secondary chemicals in the lower atmosphere, and actively used for air quality regulatory planning applications as well as for air quality forecasting for the general public health (Wong et al., 2012; Byun and Schere, 2006; Dennis et al., 2010; Rao et al., 2011; Hogrefe et al., 2001). The CTM simulation results strongly rely on two major inputs: meteorology and emissions, thus requiring accurate estimation of both to simulate the transport, chemical transformation, and removal of the pollutants. Depending on their chemical reactivity and gravitational behaviors, some pollutants can be chemically transformed and travel a long distance from their source of origin, while some are deposited near their release locations.

To accurately predict regional and global chemicals in the future, spatially and temporally resolved meteorology and emissions are critical and required to be rapidly updated based on the aerosol direct/indirect meteorology impacts within a fully coupled air quality modeling system. There have been considerable amounts of efforts in meteorology prediction enhancements actively conducted (Jacob and Winner, 2009; Grell and Baklanov, 2011; Fiore et al., 2012; Wong et al., 2012). However, there have been only limited "*inline*" emissions modeling enhancements made to CTM system wherein emissions from meteorologically driven air pollutant emission processes are dynamically coupled within the regional/global CTM modeling system, rather than being estimated *a priori* and statically provided as model inputs based on "offline" spatial and temporal allocations. Simulating emissions "*inline*" is especially crucial for real-time air quality forecasting (Tong et al., 2012). In particular, the system of the National Oceanic and Atmospheric Administration (NOAA) National Air Quality Forecast Capability (NAQFC) allows to induce the influences of the forecast meteorology on emissions from key sources, such as stationary power plants, vegetation, fertilizer applications, such as mineral dust (Knippertz and Todd, 2012), sea salt (Foltescu et al., 2005; Pierce and Adams, 2006), biogenic volatile organic compounds (BVOCs) (Lathière et al., 2005; Chen et al., 2018), and biomass burning events (Grell et al., 2011; Pavlovic et al., 2016). Despite these scientific advancements and model improvements, true process-based interaction between local meteorology and meteorology-induced anthropogenic pollutant emissions from onroad vehicles, livestock wastes, and residential heating remain incomplete or overlooked (Pouliot, 2005; Tong et al., 2012).

The mobile/transportation sector is one of the most important anthropogenic emissions sectors in metropolitan regions where most of high ozone and $PM_{2.5}$ concentration episodes often occur (Andrade et al., 2017; Kumar et al., 2018; Perugu, 2019). It is also known that the performance and emissions of mobile engines are sensitive to local weather conditions, such as ambient temperature and humidity (Lindhjem et al., 2004; Iodice and Senatore, 2014; Choi et al., 2017; Mellios. et al., 2019). The incomplete fuel combustion can be occurred under cold ambient temperature and high humidity, leading to higher emissions emitted. The effect of humidity on internal combustion engines, including spark-ignition engines (gasoline, LPG, and natural gas) and compression ignition or diesel engines, has been known for many years, with evidence indicating that higher humidity results in lower NOx emissions (Lindhjem et al., 2004; USEPA, 2015). Additional emissions also come from energy usage of air conditioning at higher ambient temperatures. These meteorological impacts can be accounted for using the state-of-science mobile emissions models such as the U.S. EPA's MOtor Vehicle Emission Simulator (MOVES) version 3.0 (USEPA, 2020). However, it lacks

transparency of air pollutant emission algorithms, including key parameters such as emission factors. Furthermore, it requires significant computational resources to generate these high-quality spatiotemporal emissions from onroad vehicles (Li et al., 2016; Xu et al., 2016; Liu et al., 2019; Perugu, 2019). To generate the "*offline*" weather-aware onroad mobile emissions outside the current CMAQ, the MOVES has been integrated with the Sparse Matrix Operator Kernel Emissions (SMOKE) modeling system, called SMOKE-MOVES integration tool (Baek et al., 2010) by processing (reading/storing/accessing) MOVES emission factors (EF) datasets. However, it demands significant computational time and memory in the SMOKE-MOVES integration approach due to the high traffic of input/output (I/O) data, which largely prohibits its usage in real-time air quality forecasting. As an example, the latest version of SMOKE version 4.8.1 can require approximately 1.9 computing hours with up to 20GB RAM memory to generate 25 hours CMAQ-ready gridded hourly emissions over Continental U.S. (CONUS) modeling domain (12km *12km grid size) offline.

To enable the indirect/direct feedback effects of aerosols and local meteorology in an air quality modeling system without any computational bottleneck, we have developed an "*inline*" meteorology-induce emissions coupler module within the US EPA's CMAQ modeling system, called "Meteorologically-induced anthropogenic Emissions: CMAQ-MetEmis", to dynamically model the complex MOVES onroad mobile emissions inline. To address the shortcomings (computational time and memory requirements) in the current slow "*offline*" SMOKE-MOVES integration approach, we first re-restructured the SMOKE-MOVES integration tool by storing the ambient temperature-specific gridded hourly emissions into a pseudo-layer structure for easy and fast access. Each pseudo-layer holds the gridded chemically-speciated hourly emissions by incremental temperature bin (e.g., 10F, 20F, and so on). The CMAQ-MetEmis coupler was developed to estimate the gridded hourly emissions with a simple linear interpolation between two temperature-bins gridded hourly emissions based on a simulated hourly ambient temperature. With an instance interpolation calculation approach, the new "*inline*" CMAQ-MetEmis approach significantly enhances the computational efficiency compared to the existing "*offline*" SMOKE-MOVES approach without losing any accuracy of emission estimates. We also evaluate the performance of the CMAQ-MetEmis coupler module in CMAQ, which includes their computational performance, the feasibility of CMAQ-MetEmis implementation as a forecasting application, and the responses of O_3 and $PM_{2.5}$ to the meteorological impacts on anthropogenic emissions.

2. CMAQ-MetEmis Development

NOAA has developed the NAQFC, operated by the National Weather Service (NWS), in partnership with the U.S EPA using the state-of-science air quality modeling system, CMAQ, to forecast concentrations of O_3 and $PM_{2.5}$ over the contiguous continental U.S. (CONUS), Alaska and Hawaii (Tong et al., 2015; Lee et al., 2017; Tang et al., 2017). Unlike weather forecasting, air quality forecasting requires full atmospheric chemistry along with the physical state and tendency of the weather in the near future. Accurate prediction of meteorology and emissions for CMAQ plays a critical role in the accuracy of 48- and 72-hour air quality forecasting. The current NOAA/NWS operational requirements specify that the post-processing of the simulated/forecasted meteorological data, emission data, and air quality chemistry model simulations be completed in a reasonable time frame to meet the air quality forecasting time constraints. Since the processing of the meteorological data and the execution of the air quality chemistry model are the most time-consuming part of CMAQ, minimizing the processing time of the emissions needs is desirable. A typical emission-processing over U.S. CONUS national domain for one day may take up to 2 hours on a single CPU

(Intel Xeon Gold 6240R @ 2.4GHz) using SMOKE and other emission post-processing tools. To expedite the operational forecasting streamlines, non-meteorological dependent emissions are generally processed in advance (Tong et al., 2015). Only the meteorologically induced emission sources are processed during the air quality forecasting simulation runs. So then, the accuracy of the emission processing can be maintained, and the forecast can be completed within the required time constraints.

2.1 Meteorology-Induced Mobile Emissions

Mobile emissions from onroad and off-network (e.g., vehicle start-up, running exhaust, break-tire wear, hot soak, and extended idling) are sensitive to temperature and humidity due to various factors, 1) cold engine starts that enhance emissions at lower ambient temperatures due to the incomplete fuel combustion, 2) evaporative losses of volatile organic compounds (VOCs) due to expansion and contraction caused by ambient diurnal temperature variations, 3) enhanced running emissions at higher ambient temperatures, 4) atmospheric moisture suppression of high combustion temperatures that lower nitrogen oxide emissions at higher humidity, and 5) indirect increased emissions from air conditioning at higher ambient temperatures (Choi et al., 2017; Iodice and Senatore, 2014; Lindhjem et al., 2004; Mellios. et al., 2019; USEPA, 2015). McDonald *et al*. (2018) found that NOx emissions from NEI estimated from the U.S. EPA's MOVES are underestimated, leading to a failure of prediction of high ozone days (8-hr max ozone>70 ppb). (McDonald et al., 2018)

The dependency of mobile emissions on local meteorology can vary by vehicle types (light-duty, heavy-duty, truck and bus), fuel types (gasoline, diesel, hybrid, and electric), road types (interstate, freeway, local roads), processes (vehicle start-up, running exhaust, break-tire wear, hot soak, and extended idling), vehicle speed for onroad vehicles, hour of the day for off-network vehicles, as well as by pollutants such as CO, NO_X, SO_2, NH_3, VOC, Particulate Matter (PM). Figure 1 shows the dependency of MOVES emission factors of CO, NOx, VOC, and $PM_{2.5}$ from gasoline-fueled vehicles on ambient temperature from onroad and off-network, respectively. All pollutant emissions vary with the temperature, particularly under lower speeds. The CO, VOC, and NOx emissions increase with the temperature while the opposite relationship is suggested between $PM_{2.5}$ emissions and temperature, implying the complexity of meteorology impacts on different pollutant emissions. For off-network emissions from gasoline-fueled vehicles, CO, NOx, and $PM_{2.5}$ show negative correlations with temperature, while the VOC exhibits a nonlinear response to the temperature variation. The largest meteorology dependency occurs in the daytime when emissions are the greatest. Further detailed meteorology dependency of MOVES emission factors on local meteorology can be found in Choi *et al*., 2017.

2.2 SMOKE-MOVES Integration Tool

In 2010, U.S. EPA introduced the process-based onroad mobile emissions model, MOVES, which is a state-of-the-science MySQL database-driven software for calculating bottom-up vehicular emissions from onroad and off-network. Depending on its application, the MOVES can generate onroad mobile emissions in two different modes. The "Inventory Mode" can generate the county-level monthly total emissions inventory, while the "Emission Rates Mode" can generate the complex emission rates, which are a function of local meteorological variables, such as ambient temperature and humidity. They play a key role in the emissions from vehicles on the roads. The county total emissions inventory in a unit of tons/month or tons/year from the "Inventory Mode" can be directly processed through the SMOKE modeling system with the static temporal allocation profiles (e.g., weekly and diurnal profiles) to generate the CMAQ-ready gridded hourly emissions. However, the "Emission Rates Mode" can generate the complex emission factors for SMOKE to

dynamically estimate the temporally and spatially enhanced onroad mobile emissions with the simulated meteorology inputs. Unlike the "Inventory Mode," the "Emission Rates Mode" MOVES runs can take up to 30 hours to generate the detailed emission factors for each county. MOVES can generate the emission factors for off-network emission processes (e.g., parked engine-off, the engine starts, idling, and fuel vapor venting), which are hour-dependent due to vehicle activity assumptions built into the MOVES model; the emission rate in a unit of grams/mile/hour depends on both hours of the day and temperature. It can also generate detail emission factors for onroad emission processes (e.g., running exhaust, crankcase running exhaust, brake wear, tire wear, and on-road evaporative), on the other hand, do not depend on the hour but are expressed in grams/mile.

MOVES is approved for use in any official state implementation plan (SIP) submissions to U.S. EPA and for conformity emissions inventory development outside of California. Furthermore, it can be used to estimate onroad vehicle emissions for a variety of different purposes: to evaluate the national and local emissions trends, to compare different emission scenarios, to analyze the benefits of mobile source control strategies, and to provide inputs for air quality modeling. Although MOVES estimates of mobile emissions include the dependence on vehicle activities and simulated hourly meteorology, its computational requirements are prohibitive in real-time air quality forecasting applications. The dynamic "*offline*" SMOKE-MOVES tool was developed by integrating MOVES emission factor (EF) outputs with the SMOKE modeling system prior to the CMAQ simulation (Baek, 2010), with the objective of improving the accuracy of mobile emissions for air quality modeling applications. The tool can dynamically estimate hourly mobile emissions based on vehicle activity inventories (i.e., miles traveled, population, and operating hours), MOVES EFs (a function of vehicle type, road type, and local meteorology), and simulated hourly ambient temperatures, and humidity. It first estimates spatially and temporally averaged county-level hourly meteorological inputs (temperatures and humidity). It then prepares driver and post-processing scripts to set up and run MOVES to generate county-specific MOVES EF lookup tables (LUT), and to sort them by average vehicle speed, ambient temperatures, humidity, operating hours, day of the week, and/or hour of the day. Finally, the tool runs a SMOKE program called "*Movesmrg*" designed to process the MOVES EF LUTs to estimate air quality model-ready gridded hourly emissions with simulated hourly meteorology (Figure 2a).

Based on the latest 2017 National Emissions Inventory (NEI) Emissions Modeling Platform (EMP) (USEPA, 2022), the SMOKE-MOVES integration tool processes over 668 county-level MOVES EF LUT files (334 files per season) ranging from 60MB up to 150MB to model over 3,100 counties in their modeling domain (e.g., 12kmx12km grid over U.S. Continental) which requires significant computational resources, such as memory, computing time (> 1.9 computing hours for 25 hours processing), and storage spaces. The SMOKE-MOVES integration step for the onroad mobile emission sector requires the most computational time, and it is not feasible for us to implement it into the current NAQFC forecasting system, which will significantly delay its processing time due to its computational resource requirement. Details on its computational requirements will be described in later section.

2.3 MetEmis Dynamic Coupler

Although the current "*offline*" SMOKE-MOVES integration tool can estimate weather-aware onroad mobile emissions for CTMs using their local meteorology, it is not fully coupled with CTM to dynamically provide aerosol direct/indirect feedback to climate and meteorology, and to enhance the air quality forecast modeling applications in seasonal-to-sub seasonal predictions due to its slow computation process.

In this study, we developed the Meteorologically-induced Emissions coupler module (MetEmis) within the CMAQ modeling system to enhance the current NAQFC with the weather-aware emissions modeling capability without any computational burden to the system. Pouliot (2005) indicated that the main obstacle to implementing weather-aware mobile emissions into air quality simulation is a significant computational resource requirement, especially for air quality forecasting applications. To address these potential shortcomings (computational time and memory requirements) without compromising any accuracy compared to the current "*offline*" SMOKE-MOVES integration tool, we first implemented a new optional feature in the *Movesmrg* program in the SMOKE v5.0 modeling system to generate the temperature-specific pre-gridded hourly emissions called "MetEmis_TBL" that holds them into the pseudo-layer structure for easy and fast access for later weather-aware emissions coupler (Figure 2). Each pseudo-layer holds the pre-gridded hourly emissions based on pre-defined temperature bins (e.g., 5°C, 10°C, 15°C, and so on). Thus, the single MetEmis_TBL file that holds both fuel months (January-Winter and July-Summer) can replace the entire MOVES EF LUT files for SMOKE and CMAQ modeling system to generate the CTM-ready weather-aware mobile emissions.

There are two ways to process the "MetEmis_TBL" emissions output file from the SMOKE (*Movesmrg)* to develop weather-aware emissions easier and faster: (a) "SMOKE-MetEmis", and (b) "CMAQ-MetEmis". The "SMOKE-MetEmis" is an "*offline*" approach which is practically the same as the SMOKE-MOVES integration other than processing the MetEmis_TBL emissions file, instead of over 668 ASCII-formatted MOVES EF LUTs files from MOVES. Both SMOKE-MetEmis and SMOKE-MOVES approaches generate identical "*offline*" gridded hourly emissions prior to the CMAQ simulations, but the SMOKE-MetEmis is significantly faster (Figure 2a). The updated *Mrggrid* utility tool from the SMOKE v5.0 will first read and process the "MetEmis_TBL" emissions file with the simulated forecast meteorology prior to the CMAQ simulations. However, the "CMAQ-MetEmis" is a true "*inline*" approach based on the CMAQ version 5.3.2 with a new dynamic emission coupler module called "MetEmis" that can generate weather-aware emissions with "MetEmis_TBL" within the CMAQ simulations (Figure 2b). It means that it can be dynamically coupled to estimate weather-aware emissions "*inline*" without any computational burdens under the CMAQ parallelized simulations. The details of computational enhancements are discussed in next section.

2.4 MetEmis Computational Efficiency

While estimating meteorologically-induced onroad mobile emissions using local meteorology accurately provides the emissions to CTM, the current "*offline*" SMOKE-MOVES integration tool approach has faced many challenges, such as computational burdens, and the data portability and distributions due to the size of data files and computationally expensive I/O data processing. Accurately generating the onroad mobile emissions for the U.S. continental using MOVES onroad emission model requires a significant amount of computational resources as well as processing time. It takes approximately 12 computing hours to generate one county MOVES EF LUT table per month using MOVES (Baek et al., 2010). Simulating over 3,100 counties in the U.S. continental (CONUS) for 12 calendar months (>37,400 MOVES simulations) will require a tremendous amount of computational resources and time. Thus, U.S. EPA has adopted the representative county approach to reduce the number of counties as well as the number of modeling months. Each representative county was classified according to its state, altitude (high or low), fuel region, the presence of inspection and maintenance programs, the mean light-duty age, and the fraction of ramps (CRC, 2019). A total of 296 representative counties for CONUS and 38 for Alaska, Hawaii, Puerto Rico, and the

US Virgin Islands (USEPA, 2022). Each representative county holds two fuel months to represent all 12 calendar months.

55   To generate one day (25 hourly time steps) CMAQ-ready gridded hourly emissions, SMOKE needs to read and process 334 MOVES EF LUT as well as many other SMOKE-ancillary input files such as VMT activity, temporal profiles, chemical speciation profiles, spatial surrogates, and so on. The most computational resources are consumed in I/O (inputs and outputs) of huge amount of data files while it processes the complex datasets. Table 1 shows the estimated computational resources and time per each onrad mobile

60   sector (e.g., RatePerDistance (RPD), RatePerVehicle (RPV), and RatePerHour (RPH)). Among the mobile sectors, RPD and RPV are the slowest sectors processed in the SMOKE modeling system. Each mobile sector contains a total of 668 MOVES LUT files (334 counties × 2 fuel months), and a total of 2004 (=668 × 3 sectors) MOVES LUT files are processed to generate the mobile sector-specific CMAQ-ready gridded hourly emissions.

65   Based on the latest 2017 NEI EMP, CMAQ-ready gridded hourly emissions in our modeling domain (e.g., 12×12km grid over U.S. Continental) requires approximately 1.9 hours per day (RPD: 90 minutes, RPV: 18 minutes, and RPH: 1 minute) to generate the complete set of onroad mobile daily emissions including RPD, RPV and RPH modes. It may require over 638.5 hours (~29 days) of computational time to generate CONUS gridded hourly emissions for 365 days. While the CMAQ-MetEmis "*inline*" approach (Figure 2b) does not

70   cause much computational processing time since the I/O of NetCDF/IOAPI binary format MetEmis_TBL input file in the CMAQ modeling system is instantaneous. There was less than 1 minute per day of CMAQ computational time with 96 CPUs of parallel processing.

The latest version of SMOKE can generate a single MetEmis_TBL output file as an option. It can hold the 25 temperature-bins gridded hourly emissions for 334 representative counties for one fuel month from 0^oF

75   to 125^oF temperature (25 bins with 5^oF increment). Correction equations for humidity are applied to estimate grid-cell-hour adjustment factors for NO_x emissions by fuel type (USEPA, 1997). Because onroad sectors (e.g., RPD, RPV, and RPH) share the same linear interpolation to estimate the emission factors between two temperature bins from the MOVES LUT files, the sector-specific MetEmis_TBL files can be merged and represent all sectors with one-time interpolation through SMOKE-MetEmis and CMAQ-MetEmis modules.

80   Thus, the merged MetEmis_TBL file can represent the entire U.S. with 334 representative county-specific MOVES LUTs files per fuel month with 25 temperature bins. The size of MOVES_TBL is approximately 16GB which is significantly smaller than the size for all 2004 MOVES LUTs files for all RPD, RPV, and RPH sectors, which is ~ 97.3 GB (62.8GB+34.5GB+48MB) (Table 1). Approximately 6 hours are required to generate the MetEmis_TBL file once with SMOKE per fuel month, prior to the CMAQ-MetEmis

85   simulations. This MetEmis_TBL can hold more than a single fuel month with the increased file size, and replace the entire 2,004 MOVES LUT files (~97.3GB) for both fuel months (e.g., January-Winter and July-Summer) with the single MetEmis_TBL file (~16GB). The final merged MetEmis_TBL file is portable and can be a direct input to CMAQ-MetEmis coupler in the CMAQ modeling system.

3. Results

90   The CMAQ air quality modeling runs are configured close to the current operational NAQFC, including the spatial coverage, emission inputs, and chemical transport model. It contains three major components: meteorology, emission, and chemical transport models. The Weather Research and Forecasting (WRF) model version 4.2.1 (Skamarock et al., 2005) is used to generate hourly meteorological fields to drive emission and air quality modeling. The WRF model was configured with Morrison 2-moment microphysics

95   scheme, RRTMG long and short-wave radiation scheme, YSU PBL scheme, Pleim-Xiu land-surface

model, Revised MM5 (Jimenez) surface layer scheme, and GF with radiative feedback cumulus parameterization option. The emission input was provided using a hybrid emission modeling system that utilized the SMOKE model version 4.8.1 (Baek and Seppanen, 2021) to process anthropogenic emissions, and a suite of emission models to estimate emissions from intermittent and/or meteorology-dependent sources. Anthropogenic emissions were taken from US EPA 2017 NEI EMP. The CMAQ model (version 5.3.2) ingests emissions and meteorology to predict spatial and temporal variations of the atmospheric pollutants (such as O_3, NO_2, and particulate matters) using a revised Carbon Bond 6 gas-phase mechanism and AE7 aerosol mechanism (CB6r3_AE7_AQ) (Byun and Schere, 2006; Luecken et al., 2019).

The meteorological, emission, and air quality models have 12×12 km horizontal resolution over the contiguous United States, with full 35 sigma layers vertically and the domain top at 50 hPa. The WRF model was driven by the forecast fields of Global Forecast System (GFS) version 4 products with a horizontal resolution of 0.25° × 0.25° (available every 6 h) and was reinitialized every 24 hour to be consistent with its operational task.

To understand the impacts of meteorology-induced onroad emissions on local air quality, we conducted two CMAQ simulation scenarios ("*Base*" amd "*MetEmis*"). All simulations were conducted for two months, January and July in the year 2019. We initiated our CMAQ simulations based on the default CMAQ background concentration profiles. The first three days of the CMAQ simulation were used as a spin-up modeling period to eliminate the influence of the initial condition (Chen et al., 2021; Lv et al., 2018; Tong and Mauzerall, 2006). The configurations and simulations are listed in Table 2.2

- "Base" scenario: Static offline approach-based (no-weather-aware) gridded hourly emissions based on the county total emissions with static temporal profiles (monthly, weekly, month-to-day, and hourly).
- "MetEmis" scenario: Dynamic inline approach-based weather-aware gridded hourly emissions dynamically estimated with simulated meteorology using the *inline* "CMAQ-MetEmis" approach.

The monthly total emissions inventories used in the "Base" scenario are based on the MOVES "Inventory Mode" simulation with monthly average ambient temperature and humidity, while the MOVES "Emission Rates Mode" simulation was used for the "MetEmis" scenarios with the simulated hourly temperature and humidity. In order to evaluate the impact of the "MetEmis" approach, we analyze the response of NOx, VOC, NH3, and PM2.5 emissions to the dynamic "*inline*" MetEmis coupler approach. The evaluation of the CMAQ-MetEmis air quality modeling system was performed by the comparison of the simulated ambient concentrations of NO_2, O_3, and PM2.5 with the observations where most of the meteorology-induced emissions are impacted by the meteorology compared to the static "offline" approach (i.e, Base). Note that both "Base" and "MetEmis" onroad mobile emissions are from the 2017 NEI EMP package.

3.1 Weather-Aware Mobile Emissions

The huge computational burden of the traditional "*offline*" SMOKE-MOVES approach prohibits its usage in providing real-time estimates of mobile emissions, which might be significantly driven by weather changes, resulting in considerable uncertainties in predicting emissions and air quality. The spatial monthly total difference plots of VOC and NOx between "Base" and "MetEmis" from Figure 3 clearly show that most of the emission differences caused by local meteorology occur from major interstate roads and metropolitan cities (e.g., New York, Detroit, Chicago, Los Angeles, Phoenix, and Atlanta), where onroad mobile emissions contribute the most. Especially, the most differences in VOC occurred over California region in July 2019, probably because the original temporal profiles assumed in "Base" are not suitable to represent the real

40   condition influenced by the weather. The January and July VOC emissions from the "Base" scenario were higher by over 8% and 20% than the ones from the "MetEmis" scenarios, respectively, indicating that current NAQFC-ready onroad mobile emissions (no-weather-aware) are significantly over-representing the VOC emissions compared to the weather-aware VOC dynamically estimated by MetEmis.

Unlike the "Base" approach, the "MetEmis" approach estimates hourly emissions by multiplying the
45   estimated hourly vehicle mileage traveled (VMT) in the unit of miles/hour with inventory pollutant emission rates (unit of grams/miles), which are a function of local meteorology (e.g., ambient temperature and humidity). The "MetEmis" emissions can enhance their spatiotemporal representations of onroad mobile sources. However, the hourly VMT activity data is estimated using the same temporal profiles used in the "Base" hourly emissions. Thus, both onroad emissions follow similar weekly and daily patterns with some
50   hourly variations based on local meteorological conditions. As presented in Figure 4, which compares the hourly domain total TOG (Total Organic Gases), NOx, and $PM_{2.5}$ emissions between the "Base" and the "MetEmis" approach, the statically estimated "Base" hourly emissions (colored blue) clearly show the repeated weekly patterns within the same month due to the usage of the static weekly temporal profiles, while the "MetEmis" (colored in red) display irregular hourly patterns due to the impacts of local hourly
55   meteorology.

Due to the influence of local meteorology (i.e., ambient temperature and humidity), the onroad running exhaust/evaporative emissions, and the off-network evaporative emissions show a moderate decrease of TOG and a slight increase of NOx (> 4% increase) over the entire domain due to low ambient and humidity condition during the winter season (January), according to "MetEmis" estimates. The most important
60   enhancement in the "MetEmis" approach is allowing modelers to simulate NAQFC-ready weather-aware onroad mobile emissions. More importantly, the daily differences are also noticeable in the "MetEmis" approach within one month, as higher TOG and $PM_{2.5}$ are shown in late January due to the increased temperature, while the "Base" approach failed to predict such variation. Such spatiotemporal enhancements of onroad mobile emissions predicted by "MetEmis", especially near metropolitan regions, would benefit the
65   NAQFC. As stated, these onroad mobile emissions from two scenarios are based on the MOVES simulations designed for the 2017 NEI EMP.

3.2 Weather-Aware Mobile Emissions Impacts on CTM Simulations

Domain-level Evaluations
70   This study investigated the response of NO_2, O_3, and $PM_{2.5}$ to the meteorology-induced mobile emission changes by simulating air quality under two scenarios (Base and MetEmis). The sensitivity of air pollutant concentrations to these meteorology-induced emission sources was performed and analyzed in this section. The monthly statistical modeling evaluation metrics for these two simulations (Base and MetEmis) over the CONUS domain are provided in Table 3. The correlation coefficient (CORR) of O_3 is 0.51 for both
75   simulations, and they have the same normalized mean bias and errors (NMB and NME), while the relative mean square error (RMSE) of Base (7.03 ppb) is slightly higher than that of MetEmis (7 ppb). The simulated NO_2 shows the best correlations (0.64) among these three pollutants in January, however, its RMSE, NMB, and NME are the largest. The $PM_{2.5}$ simulation didn't reproduce the variability very well with a lower CORR of 0.46, but it presents the best RMSE and moderate NMB/NME. In July, the CORRs
80   of O_3 improved from 0.51 to 0.64, while the RMSEs are also increasing because of intense concentration in summer. The NO_2 and $PM_{2.5}$ have the opposite pattern of O_3 with decreased CORR (0.51 and 0.38, respectively) and improved biases and errors, except the NME of NO_2. Over the entire modeling domain, both simulations show quite similar modeling performances against the observations, with the difference generally below 1%. This is mostly attributable to the spatial pattern of emissions primarily concentrated

85   in urban areas. The most impacts of MetEmis emissions are shown over metropolitan cities where mobile emissions play a critical role in their local air quality.

Figure 5 shows the monthly average NO_2, O_3, and $PM_{2.5}$ concentrations from the Base scenario and the monthly average difference between the Base and MetEmis scenarios in July 2019. The spatial distributions of simulated NO_2 present a close pattern with those of NO_x emission in both months, demonstrating the

90   effect of local NO_x emission on the NO_2 activities. The NO_2 concentration in July is lower than in January, caused by the stronger NO_2 photolysis and ventilation. In January, the NO_2 simulated by MetEmis showed a higher concentration over the domain with more than 0.2 ppb larger over urban areas because of the increased NO_x emission after adjustment. In comparison, the monthly simulated NO_2 concentrations with and without emission adjustment are much closer in July, the emission adjustment makes the concentration

95   increase in the east while a decrease in the west. Compared to NO_2, the secondary O_3 and $PM_{2.5}$ formation chemical reactions involve complex nonlinear processes under various meteorological conditions and precursor emissions. Despite their complexity, there are strong correlations between their nonlinear responses and precursor emission changes.

City-level Evaluation

00   The O_3 concentration is generally below 36 ppb in most areas in January because of the cold weather and weak photolysis process, while it presents high over the mid-western US, which is caused by the higher altitude over the Rocky Mountains area. The O_3 significantly increases in July with an average concentration of 43.9 ppb, 10 ppb larger than that in January. In July, the northeastern US becomes the hot spot zone as the

05   local anthropogenic emission and pollution transport are strong. Meanwhile, the O_3 is also concentrated over the water, such as Great Lake and northeastern coastal areas. Most of the ozone increase occurred around the surrounding regions of metropolitan cities like Chicago, IL, Atlanta, GA, Denver, CO, and Pheonix, AZ, where both NOx and VOC emissions slightly increased during July 2019 (Figure 3). However, the San Jose area showed a significant decrease in ozone during the summer of 2019 due to the higher VOC estimations

10   from NEI (Base) compared to the ones from the MetEmis scenario (Figure 3).

The $PM_{2.5}$ simulation has similar patterns in January and July, with more particles concentrating in the east. The southwestern areas show less particulate pollution as our emissions do not include natural sources such as dust storms and wildfires. The results from MetEmis present slightly higher $PM_{2.5}$ in the east because of the increased primary $PM_{2.5}$ emission. In addition, a decreased $PM_{2.5}$ concentration is noted in California.

15   This may attribute to the less generated secondary aerosols as the VOC emission is significantly reduced after adjustment.

Thus, this study further examines the influence of meteorology-induced mobile emission changes on modeling performance, which is particularly important for air quality forecasting in NAQFC. 10 cities with the most changes in emissions are selected for comparison, as shown in Figure 6. In general, noticeable

20   improvement is found in NO_2 simulation with increasing R^2 in all 10 cities except Detroit. San Jose and Atlanta exhibit the largest improvement in NO_2 simulation. Apparently, the MetEmis successfully captured daily variations of mobile emissions, resulting in an improved temporal correlation. Meanwhile, the RMSEs were reduced in most of the cities (8 out of 10), suggesting the simulated biases can also be eliminated with MetEmis. Compared to NO_2, changes in O_3 and $PM_{2.5}$ are smaller due to the complex

25   reactions. However, improvement is also found in summer with increased R^2 and reduced RMSE in more than 70% of cities, though less improvement is suggested in winter. We analyzed a few episodes with the largest changes for O_3 and $PM_{2.5}$ to demonstrate such improvement.

Ozone Episodic Cases Evaluation

Based on the July 2019 CMAQ simulation between the Base and MetEmis cases, we identified the locations where the largest changes in surface ozone occurred. Especially, in July 2019, we witnessed a significant decrease in ozone over San Jose, CA, at 1:00 PM local time on July 24, 2019, while the most increase in ozone occurred over Chicago, IL, at 11:00 AM on July 5, 2019 (Table 5). Thus, we investigated these two episodes to understand the main drivers of these behaviors.

Largest Ozone Increase Episode

Figure 7 shows the spatial ozone concentrations and the differences over the Chicago region between the Base and MetEmis scenarios at 11 AM LST on July 5, 2019. While the highest ozone occurred around the south of Michigan Lake in both scenarios (Figure 7a), the largest ozone increase (~7ppb) is shown in the middle of Michigan Lake, where unfortunately, there is no AQS monitoring location (Figure 7b). To understand the cause of these ozone changes, we examined the differences in NOx and VOC emissions between Base and MetEmis scenarios. The increase of VOC emissions from the MetEmis scenario in the early morning (3LST-9LST) over the VOC-limited Chicago, IL region seems to be the main driver of a significant increase in ozone (Figure 8). The detailed information on VOC and NOx concentration changes on July 5th, 2019, is listed in Table 5. In the early morning, there was a decrease in NOx concentration and an increase in VOC concentrations over the Chicago area. Due to no monitoring location available over the lake, we could not properly perform the modeling evaluation statistics during the largest ozone increase.

Largest Ozone Decrease Episode

There was more than an 80ppb ozone decrease over San Jose, CA, at 11LST on July 24th, 2019. To understand the cause of this significant decrease, we performed the analysis of precursor emissions changes during the episode period. The colored green AQS locations are selected for the ozone concentration analysis, while the red ones are for the $PM_{2.5}$ monitoring locations (Figure 9a). Figure 9b shows the modeled hourly ozone concentrations (maximum, minimum, and mean) and AQS observations over the blue box targeted region from Figure 9a. Figure 9b and Figure 10 indicate that the maximum ozone values from the "Base" scenario clearly show an overestimated ozone over San Jose, CA downwind region, while the MetEmis case shows a significant improvement in maximum ozone concentration during the daytime. The main driver of this significant ozone change over the San Jose targeted area is due to the substantial reduction in VOC emissions in MetEmis from Base (Figure 11a). Statistics of NOx and VOC concentrations from CMAQ in Table 6 show consistent findings.

$PM_{2.5}$ Episodic Case Evaluation

Along with the significant ozone decrease in July 2019, there was a significant $PM_{2.5}$ decrease from the CMAQ-MetEmis simulation from 42.5µg/m^3 (Base) to 25µg/m^3 at 10LST on January 3, 2019. Approximately 17.5 µg/m^3 (>41%) $PM_{2.5}$ decrease was witnessed in CMAQ-MetEmis simulations (Figure 11). The CMAQ-MetEmis simulation shows a significant improvement in modeled $PM_{2.5}$ concentration, compared to the ones from the AQS monitoring locations from 8a (Figure 12a). The main cause of this $PM_{2.5}$ decrease in CMAQ-MetEmis is mainly a significant decrease in primary $PM_{2.5}$ and VOC emissions (Figure 13). Primary hourly $PM_{2.5}$ emissions from the MetEmis scenario were significantly lowered than the ones from the Base scenario, approximately a maximum of 20kg/hour from 3 LST to 9 LST on January 3, 2019.

4. Conclusions

To address the limitation of traditional estimation for onroad vehicle emissions, this study developed a novel method (*i.e.*, MetEmis) by dynamically coupling the meteorology-induced onroad emissions with simulated meteorological data in the air quality modeling system, which significantly improves both computational efficiency and accuracy. The computational time for processing one-day onroad emission data is substantially reduced from 1.9 hours offline to less than 1 minute inline, enabling the onroad emission estimates simultaneously coupled with the meteorology forecasting. Overall, the MetEmis corrected the low biases of NO_x and primary $PM_{2.5}$ emissions domain-wide, and high-biases of VOC emissions in California. The MetEmis also successfully captured the temporal variation of onroad vehicle emissions, resulting in improved simulated NO_2, O_3, and $PM_{2.5}$ concentrations with more agreement with observations compared to the ones using static temporal profiles. Particularly, the simulated NO_2 concentration exhibits noticeable improvement with increased R^2 and decreased RMSEs in most cities. The simulated O_3 and $PM_{2.5}$ concentrations were also improved, particularly in summer.

The newly developed CMAQ-MetEmis model demonstrates the importance of dynamic-coupling emissions and meteorological forecasting. While this study only focused on the onroad emissions, other meteorology-induced sectors such as residential combustions and agricultural livestock are planned to be included in the MetEmis development well to represent the meteorological influence on all meteorologically-induced anthropogenic emissions. Meanwhile, this study mainly focuses on replicating the same dynamic emissions from the offline SMOKE-MOVES onroad mobile emissions for the CMAQ model as the inline option. The native uncertainties from the MOVES model still exist and may lead to the uncertainties in the temporal profile estimated in MetEmis, which need be further improved in the following studies.

Digital Object Identifier (DOI) for the CMAQ-MetEmis Coupler:

95 https://doi.org/10.5281/zenodo.7150000

Code Availability:

The source codes of the SMOKE and the CMAQ models for MetEmis coupler can be downloaded from the DOI website (https://doi.org/10.5281/zenodo.7150000)

Data availability:

00 All the datasets, excel and python scripts used in this manuscript for the data analysis are uploaded through the DOI website (https://doi.org/10.5281/zenodo.7150000)

Author contribution

Dr. B.H. Baek is the lead researcher in this study, and Drs. Baek and Coats developed the source codes of CMAQ-MetEmis. Drs. Ma, Wang, Li, Xing and Tong prepared the modeling inputs and analyzed the

05 modeling results. Drs. Woo and Kim participated in the design of the weather-aware emission modeling system.

Competing interests

The Authors declare that they have no conflict of interest.

Acknowledgments

10 This research was funded by the National Oceanic and Atmospheric Administration (NOAA)'s Office of Weather and Air Quality (OWAQ) to improve the National Air Quality Forecasting Capability (NAQFC) (Award: NOAA-OAR-OWAQ-2019-2005820) and National Strategic Project-Fine Particle of the National Research Foundation (NRF) of Korea funded by the Ministry of Science and ICT (MSIT), the Ministry of Environment (ME), the Ministry of Health and Welfare (MOHW) (NRF-2017M3D8A1092022), and by the

15 Korea Environmental Industry & Technology Institute (KEITI) through the Public Technology Program based on Environmental Policy Program, funded by Korea Ministry of Environment (MOE) (2019000160007).

References

Andrade, M. d. F., Kumar, P., de Freitas, E. D., Ynoue, R. Y., Martins, J., Martins, L. D., Nogueira, T., Perez-

20 Martinez, P., de Miranda, R. M., Albuquerque, T., Gonçalves, F. L. T., Oyama, B., and Zhang, Y.: Air quality in the megacity of São Paulo: Evolution over the last 30 years and future perspectives, Atmospheric Environment, 159, 66-82, https://doi.org/10.1016/j.atmosenv.2017.03.051, 2017.

Baek, B. H.: Integration approach of MOVES and SMOKE models, the 19th Emissions Inventory Conference, San Antonio, TX2010.

25 Baek, B. H. and Seppanen, C.: CEMPD/SMOKE: SMOKE v4.8.1 Public Release (January 29, 2021) (SMOKEv481_Jan2021): https://doi.org/10.5281/zenodo.4480334, last access: Nov 4th.

Baek, B. H., Seppanen, C., Houyoux, M., Eyth, A., and Mason, R.: Installation Guide for the SMOKE-MOVES Integration Tool, 2010.

Byun, D. and Schere, K. L.: Review of the Governing Equations, Computational Algorithms, and Other Components of the Models-3 Community Multiscale Air Quality (CMAQ) Modeling System, Applied Mechanics Reviews, 59, 51-77, 10.1115/1.2128636, 2006.

Chen, D., Liang, D., Li, L., Guo, X., Lang, J., & Zhou, Y.: The temporal and spatial changes of ship-contributed PM2. 5 due to the inter-annual meteorological variation in Yangtze river delta, China, Atmosphere, 12(6), 722, 2021.

Chen, W. H., Guenther, A. B., Wang, X. M., Chen, Y. H., Gu, D. S., Chang, M., Zhou, S. Z., Wu, L. L., and Zhang, Y. Q.: Regional to Global Biogenic Isoprene Emission Responses to Changes in Vegetation From 2000 to 2015, Journal of Geophysical Research: Atmospheres, 123, 3757-3771, 10.1002/2017jd027934, 2018.

Choi, D., Beardsley, M., Brzezinski, D., Koupal, J., and Warila, J.: MOVES Sensitivity Analysis: The Impacts of Temperature and Humidity on Emissions, 2017.

Dennis, R., Fox, T., Fuentes, M., Gilliland, A., Hanna, S., Hogrefe, C., Irwin, J., Rao, S. T., Scheffe, R., Schere, K., Steyn, D., and Venkatram, A.: A FRAMEWORK FOR EVALUATING REGIONAL-SCALE NUMERICAL PHOTOCHEMICAL MODELING SYSTEMS, Environ Fluid Mech (Dordr), 10, 471-489, 10.1007/s10652-009-9163-2, 2010.

Esri, D., HERE, TomTom, Intermap, increment P Corp., GEBCO, USGS, FAO, NPS, NRCAN, GeoBase, IGN, Kadaster NL, Ordnance Survey, Esri Japan, METI, Esri China (Hong Kong), Swisstopo, MapmyIndia, and the GIS User Community: World Topographic Map, 2013.

Fiore, A. M., Naik, V., Spracklen, D. V., Steiner, A., Unger, N., Prather, M., Bergmann, D., Cameron-Smith, P. J., Cionni, I., Collins, W. J., Dalsøren, S., Eyring, V., Folberth, G. A., Ginoux, P., Horowitz, L. W., Josse, B., Lamarque, J. F., MacKenzie, I. A., Nagashima, T., O'Connor, F. M., Righi, M., Rumbold, S. T., Shindell, D. T., Skeie, R. B., Sudo, K., Szopa, S., Takemura, T., and Zeng, G.: Global air quality and climate, Chem Soc Rev, 41, 6663-6683, 10.1039/c2cs35095e, 2012.

Foltescu, V. L., Pryor, S. C., and Bennet, C.: Sea salt generation, dispersion and removal on the regional scale, Atmospheric Environment, 39, 2123-2133, https://doi.org/10.1016/j.atmosenv.2004.12.030, 2005.

Grell, G. and Baklanov, A.: Integrated modeling for forecasting weather and air quality: A call for fully coupled approaches, Atmospheric Environment, 45, 6845-6851, https://doi.org/10.1016/j.atmosenv.2011.01.017, 2011.

Grell, G., Freitas, S. R., Stuefer, M., and Fast, J.: Inclusion of biomass burning in WRF-Chem: impact of wildfires on weather forecasts, Atmos. Chem. Phys., 11, 5289-5303, 10.5194/acp-11-5289-2011, 2011.

Hogrefe, C., Rao, S. T., Kasibhatla, P., Kallos, G., Tremback, C. J., Hao, W., Olerud, D., Xiu, A., McHenry, J., and Alapaty, K.: Evaluating the performance of regional-scale photochemical modeling systems: Part I—meteorological predictions, Atmospheric Environment, 35, 4159-4174, https://doi.org/10.1016/S1352-2310(01)00182-0, 2001.

65   Iodice, P. and Senatore, A.: Cold Start Emissions of a Motorcycle Using Ethanol-gasoline Blended Fuels, Energy Procedia, 45, 809-818, https://doi.org/10.1016/j.egypro.2014.01.086, 2014.

Jacob, D. J. and Winner, D. A.: Effect of climate change on air quality, Atmospheric Environment, 43, 51-63, https://doi.org/10.1016/j.atmosenv.2008.09.051, 2009.

Knippertz, P. and Todd, M. C.: Mineral dust aerosols over the Sahara: Meteorological controls on emission 70   and transport and implications for modeling, Reviews of Geophysics, 50, 10.1029/2011rg000362, 2012.

Kumar, P., Patton, A. P., Durant, J. L., and Frey, H. C.: A review of factors impacting exposure to PM2.5, ultrafine particles and black carbon in Asian transport microenvironments, Atmospheric Environment, 187, 301-316, https://doi.org/10.1016/j.atmosenv.2018.05.046, 2018.

Lathière, J., Hauglustaine, D. A., De Noblet-Ducoudré, N., Krinner, G., and Folberth, G. A.: Past and future 75   changes in biogenic volatile organic compound emissions simulated with a global dynamic vegetation model, Geophysical Research Letters, 32, https://doi.org/10.1029/2005GL024164, 2005.

Lee, P., McQueen, J., Stajner, I., Huang, J., Pan, L., Tong, D., Kim, H., Tang, Y., Kondragunta, S., Ruminski, M., Lu, S., Rogers, E., Saylor, R., Shafran, P., Huang, H.-C., Gorline, J., Upadhayay, S., and Artz, R.: NAQFC Developmental Forecast Guidance for Fine Particulate Matter (PM2.5), Weather and Forecasting, 80   32, 343-360, 10.1175/waf-d-15-0163.1, 2017.

Li, Q., Qiao, F., and yu, L.: Vehicle Emission Implications of Drivers Smart Advisory System for Traffic Operations in Work Zones, Journal of the Air & Waste Management Association, 11, 10.1080/10962247.2016.1140095, 2016.

Lindhjem, C., Chan, L., Pollack, A., Corporation, E. I., Way, R., and Kite, C.: Applying Humidity and 85   Temperature Corrections to On and Off-Road Mobile Source Emissions, 13th International Emission Inventory Conference, Clearwater, FL2004.

Liu, H., Guensler, R., Lu, H., Xu, Y., Xu, X., and Rodgers, M.: MOVES-Matrix for High-Performance On-Road Energy and Running Emission Rate Modeling Applications, Journal of the Air & Waste Management Association, 69, 10.1080/10962247.2019.1640806, 2019.

90   Luecken, D. J., Yarwood, G., and Hutzell, W. T.: Multipollutant modeling of ozone, reactive nitrogen and HAPs across the continental US with CMAQ-CB6, Atmospheric Environment, 201, 62-72, https://doi.org/10.1016/j.atmosenv.2018.11.060, 2019.

Lv, Z., Liu, H., Ying, Q., Fu, M., Meng, Z., Wang, Y., ... & He, K.: Impacts of shipping emissions on PM 2.5 pollution in China, Atmospheric Chemistry and Physics, 18(21), 15811-15824, 2018.

95

McDonald, B. C., McKeen, S. A., Cui, Y. Y., Ahmadov, R., Kim, S. W., Frost, G. J., Pollack, I. B., Peischl, J., Ryerson, T. B., Holloway, J. S., Graus, M., Warneke, C., Gilman, J. B., de Gouw, J. A., Kaiser, J., Keutsch, F. N., Hanisco, T. F., Wolfe, G. M., and Trainer, M.: Modeling Ozone in the Eastern U.S. using a Fuel-Based Mobile Source Emissions Inventory, Environ Sci Technol, 52, 7360-7370, 10.1021/acs.est.8b00778, 2018.

00   Mellios., G., Ntziachristos, L., Samaras, Z., White, L., Martini, G., and Rose, K.: EMEP/EEA air pollutant emission inventory guidebook 2019, Gasoline evaporation, European Environment Agency2019.

Pavlovic, R., Chen, J., Anderson, K., Moran, M. D., Beaulieu, P. A., Davignon, D., and Cousineau, S.: The FireWork air quality forecast system with near-real-time biomass burning emissions: Recent developments and evaluation of performance for the 2015 North American wildfire season, J Air Waste Manag Assoc, 66,
05   819-841, 10.1080/10962247.2016.1158214, 2016.

Perugu, H.: Emission modelling of light-duty vehicles in India using the revamped VSP-based MOVES model: The case study of Hyderabad, Transportation Research Part D: Transport and Environment, 68, 150-163, https://doi.org/10.1016/j.trd.2018.01.031, 2019.

Pierce, J. R. and Adams, P. J.: Global evaluation of CCN formation by direct emission of sea salt and growth
10   of ultrafine sea salt, Journal of Geophysical Research: Atmospheres, 111, https://doi.org/10.1029/2005JD006186, 2006.

Pouliot, G. A.: Emission processing for ETA/CMAQ, an air quality forecasting model, 7th Conference on Atmospheric Chemistry American Meteorological Society, San Diego, CA, January 09 - 13, 20052005.

Rao, S. T., Galmarini, S., and Puckett, K.: Air Quality Model Evaluation International Initiative (AQMEII):
15   Advancing the State of the Science in Regional Photochemical Modeling and Its Applications, Bulletin of the American Meteorological Society, 92, 23-30, 10.1175/2010BAMS3069.1, 2011.

Tang, Y., Pagowski, M., Chai, T., Pan, L., Lee, P., Baker, B., Kumar, R., Delle Monache, L., Tong, D., and Kim, H. C.: A case study of aerosol data assimilation with the Community Multi-scale Air Quality Model over the contiguous United States using 3D-Var and optimal interpolation methods, Geosci. Model Dev., 10,
20   4743-4758, 10.5194/gmd-10-4743-2017, 2017.

Tong, D., Lee, P., and Saylor, R.: New Direction: The need to develop process-based emission forecasting models, Atmospheric Environment, 47, 560–561, 10.1016/j.atmosenv.2011.10.070, 2012.

Tong, D., Lamsal, L., Pan, L., Ding, C., Kim, H., Lee, P., Chai, T., Pickering, K. E., and Stajner, I.: Long-term NOx trends over large cities in the United States during the great recession: Comparison of satellite

retrieals, ground observations, and emission inventories, Atmospheric Environment, 107, 70-84, https://doi.org/10.1016/j.atmosenv.2015.01.035, 2015.

Tong, D. & Mauzerall, D.L.: Spatial variability of summertime tropospheric ozone over the continental United States: Implications of an evaluation of the CMAQ model, Atmospheric Environment, 40(17), 3041-3056, 2006.

USEPA: Derivation of humidity and NOx humidity correction factors, 1997.

USEPA: Emission Adjustments for Temperature, Humidity, Air Conditioning, and Inspection and Maintenance for on-Road Vehicles in MOVES2014, 2015.

USEPA: MOVES and Other Mobile Source Emissions MOdel: https://www.epa.gov/moves, last

USEPA: 2017 Emissions Modeling Platform (EMP): https://www.epa.gov/air-emissions-modeling/2017-emissions-modeling-platform, last access: Nov 03.

Wong, K. W., Tsai, C., Lefer, B., Haman, C., Grossberg, N., Brune, W. H., Ren, X., Luke, W., and Stutz, J.: Daytime HONO vertical gradients during SHARP 2009 in Houston, TX, Atmospheric Chemistry and Physics, 12, 635-652, 10.5194/acp-12-635-2012, 2012.

Xu, X., Liu, H., Anderson, J. M., Xu, Y., Hunter, M. P., Rodgers, M. O., and Guensler, R. L.: Estimating Project-Level Vehicle Emissions with Vissim and MOVES-Matrix, Transportation Research Record, 2570, 107-117, 10.3141/2570-12, 2016.

Tables

Table 1. The required computational memory and time in the SMOKE modeling system.

Sector	Individual File Size	Total File Size (668 counties)	CPU Memory Usage (GB)	CPU Computing Time*
RPD	50~160 MB	62.8 GB	10~20	~ 90 mins/day
RPV	26~89 MB	34.5 GB	5~10	~ 18 mins/day
RPH	7~94 KB	43.6 MB	1~2	~ 1 mins/day
Total	7KB~160MB	97.3 GB	1~20	~ 110 mins/day

* The specification of CPU is Intel Xeon Gold 6240R @ 2.4GHz

50   Table 2. CMAQ modeling domain and configurations.

	Base	MetEmis
Horizontal Resolution	12km x 12km	
Meteorology	WRFv4.0 with Global Forecasting System (GFS) acting as ICs/BCs, RRTMG short/long wave scheme, PX land-surface scheme, YSU boundary layer scheme, Revised MM5 surface layer scheme, GF with radiative feedback cumulus parameterization	
Boundary Condition	GEOS monthly product	
Initial Condition	CMAQ restart file	
Chemistry	CMAQv5.3.2 CB6r3 AE7	
Emissions	2017 NEI: Onroad monthly emissions	2017 NEI: Onroad Meteorology-induced emissions

Table 3. Statistical metrics between observed and simulated O_3, NO_2 and $PM_{2.5}$ in January and July, 2019 over contiguous United States

	January 2019						July 2019					
	O_3		NO_2		$PM_{2.5}$		O_3		NO_2		$PM_{2.5}$	
	Base	MetEmis	Base	MetEmis	Base	MetEmis	Base	MetEmis	Base	MetEmis	Base	MetEmis
CORR	0.51	0.51	0.64	0.64	0.46	0.46	0.64	0.64	0.51	0.51	0.38	0.38
RMSE	7.03	7.00	8.33	8.27	5.72	5.76	9.56	9.51	5.69	5.67	5.03	5.04
NMB	-0.01	-0.01	-0.32	-0.30	0.10	0.11	-0.01	-0.01	-0.15	-0.15	-0.05	-0.05
NME	17%	17%	52%	52%	46%	47%	17%	17%	62%	62%	40%	40%

55

60

Table 4. The largest differences of ozone episodes in July 2019 over the U.S.

Episodes	Date @ Time	Base (ppb)	MetEmis (ppb)	Location
Largest Increase	Jul 5, 2019 @ 1PM	78.3	85.9 (+7.1)	Chicago, IL
Largest Decrease	Jul 24, 2019 @ 11AM	112.9	31.0 (-81.9)	San Jose, CA

65

Table 5. Summary of precursor (NOx and VOC) concentrations in the morning before the largest ozone increase episode at 14LST on July 5th, 2019 over Chicago, IL.

Jul 5th, 2019	NOx (ppb)				VOC (ppbC)			
	Time	Base	MetEmis	Diff (M-B)	Time	Base	MetEmis	Diff (M-B)
Mean	5-11AM	8.4	8.6	0.2	5-11AM	62	66	4.0
Max	6-7AM	18.9	20.7	1.8	6-7AM	101	121	20.0
Min	6-7AM	8.5	8.2	-0.3	10-11AM	74	73	-1.0

70

Table 6. Statistics of largest ozone decrease episode (July 24th, 2019) over San Jose, CA.

675

Jul 24th, 2019	NOx (ppb)				VOC (ppbC)			
	Time	Base	MetEmis	Diff (M-B)	Time	Base	MetEmis	Diff (M-B)
Mean	3-9AM	5.8	6.8	1.0	3-9AM	184	35	148
Max	10-11AM	9.0	22.0	13.0	8-9AM	1263	68	-1195
Min	11-12pM	10.8	10.6	-0.2	12PM-1AM	7.8	7.3	-0.5

Figures
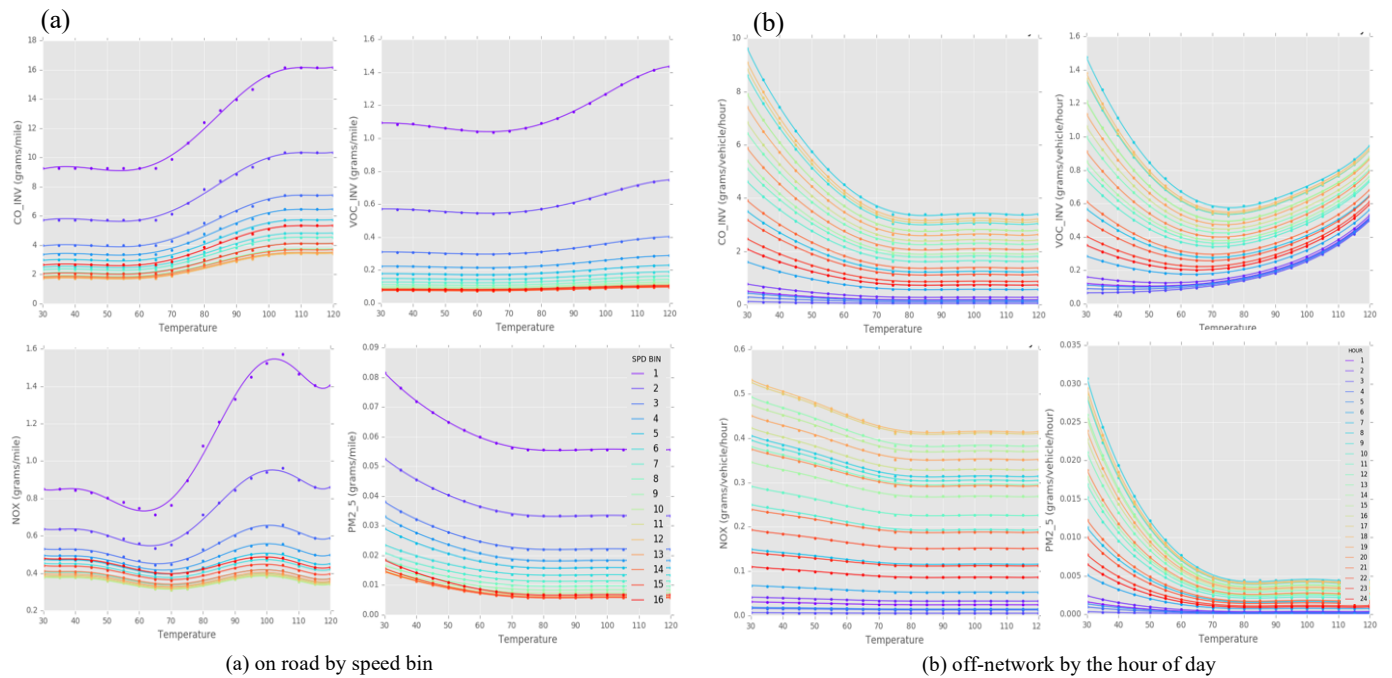
Figure 1. Meteorology-dependency of CO, VOC, NOx, and PM$_{2.5}$ emissions from gasoline-fueled light-duty vehicles by average speed bin (a), and the off-network by the hour of day (b).

80

85
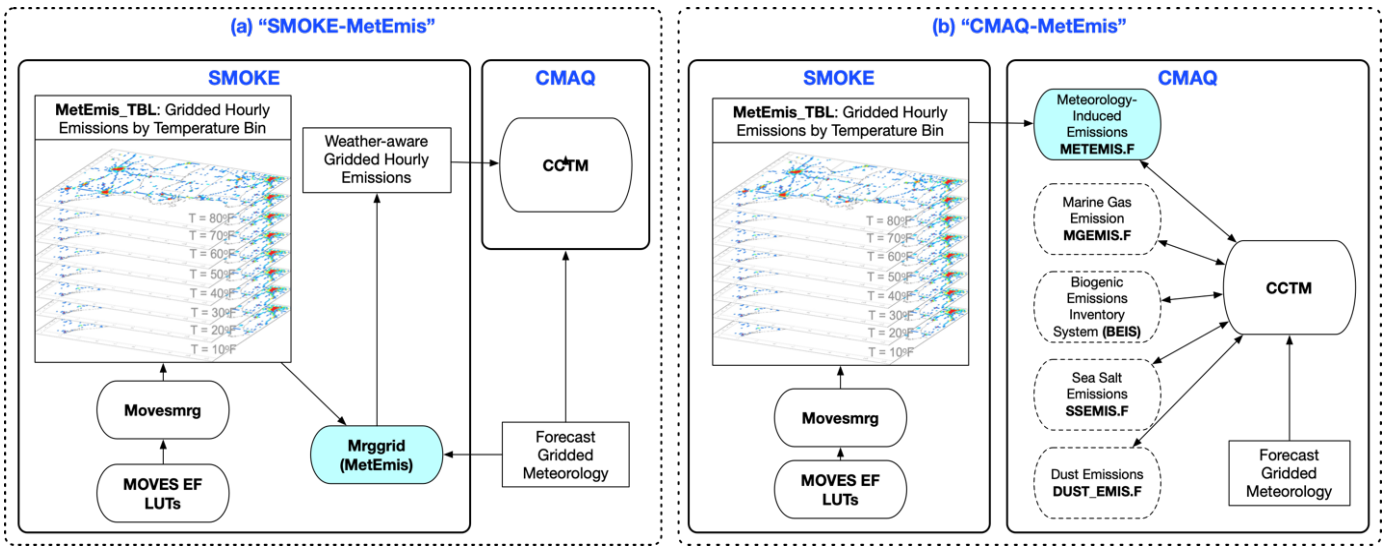
Figure 2. Meteorological-Induced Emissions coupler module "MetEmis" with air quality modeling system: a) "SMOKE-MetEmis", and b) "CMAQ-MetEmis".
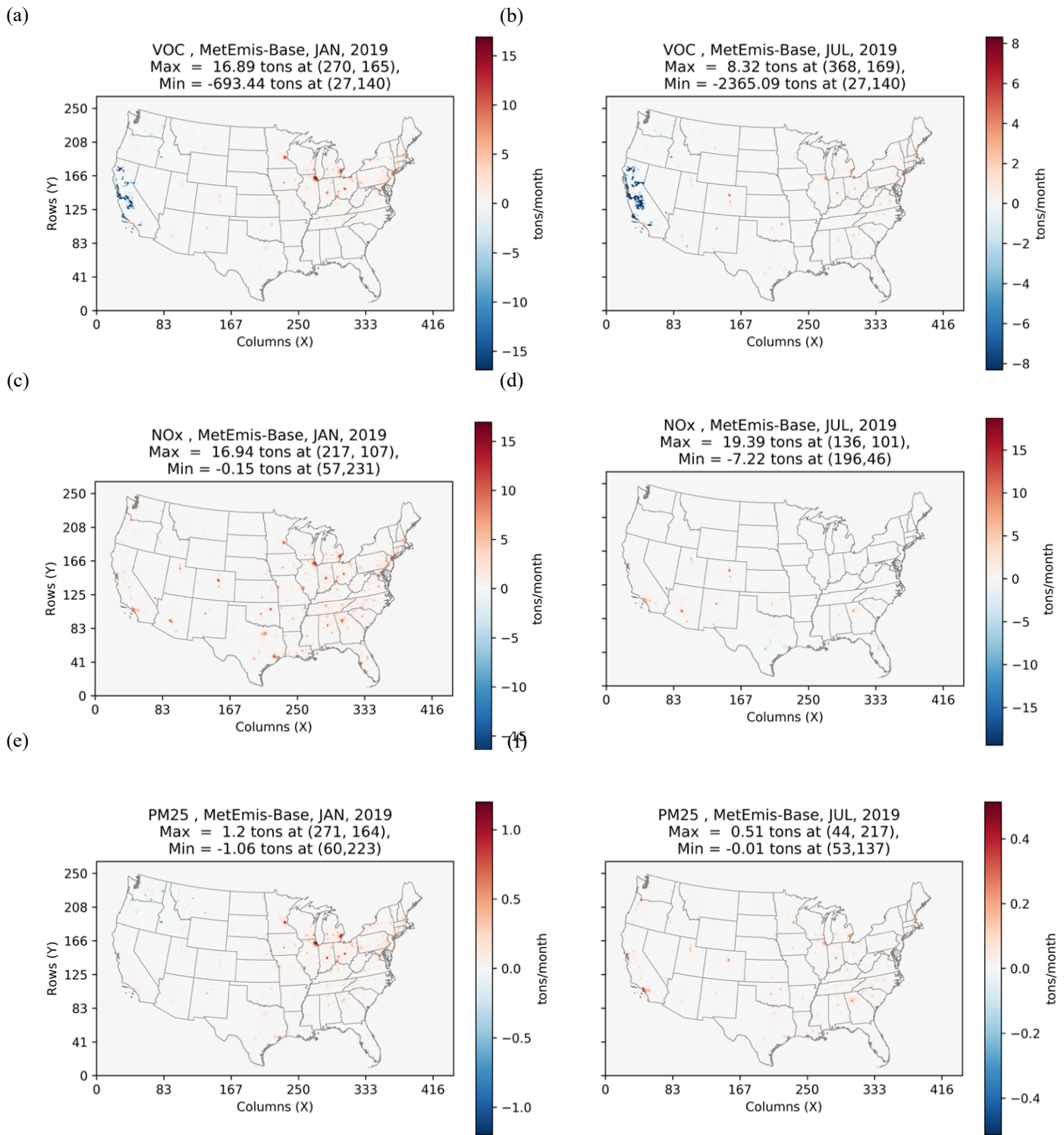
Figure 3. Spatial comparison of monthly total emissions of VOC, NO, and PM2.5. The colors indicate the MetEmis is larger than Base (red) or smaller (blue) for (a) VOC in January, (b) VOC in July, (c) NO$_X$ in January, (d) NOx in July,(e) PM2.5 in January and (f) PM2.5 in July.

90
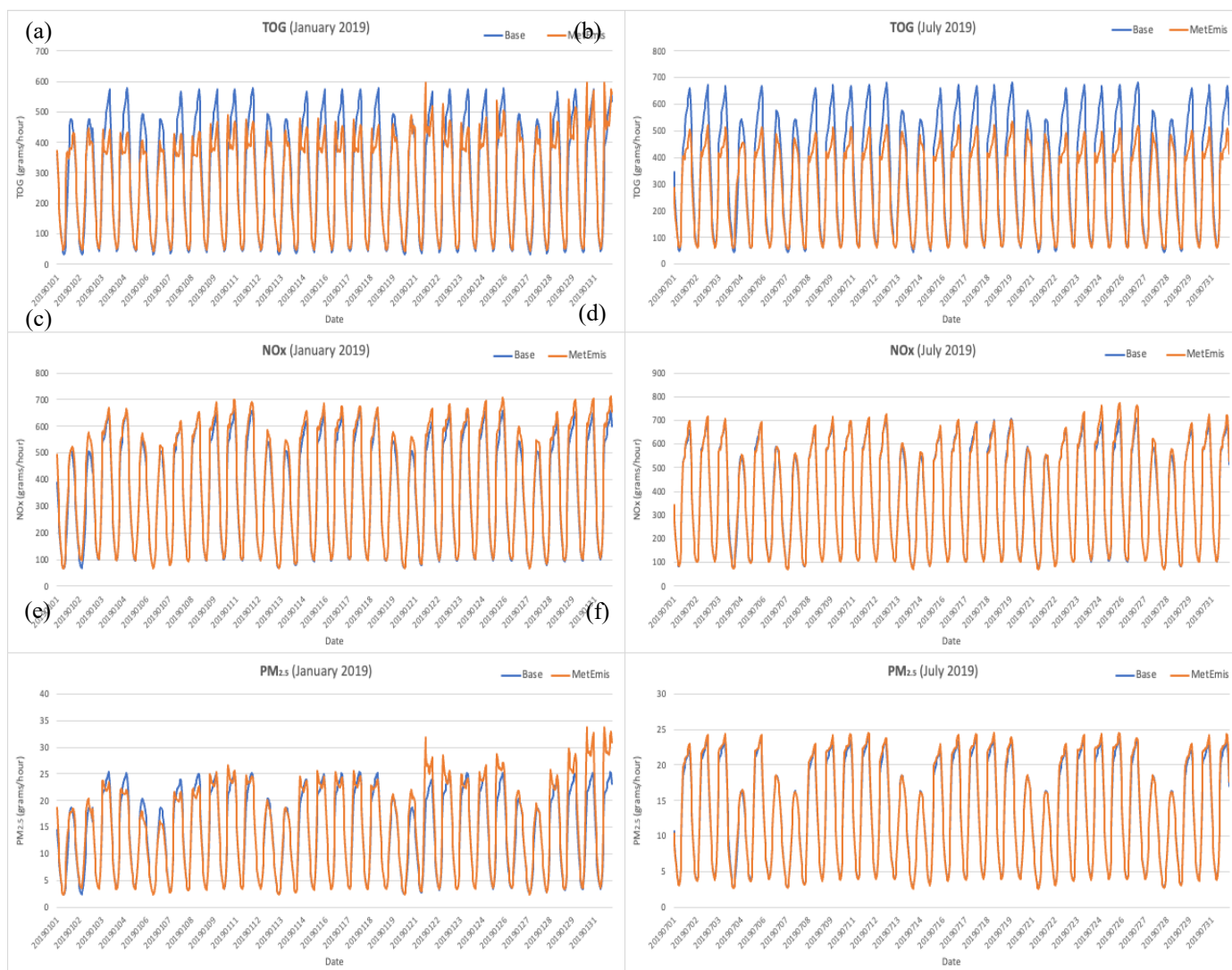
Figure 4. Temporal comparisons of daily domain total emissions of (a) Total Organic Gas (TOG) in January, (b) TOG in July, (c) NO$_X$ in January, (d) NOx in July,(e) PM$_{2.5}$ in January and (f) PM$_{2.5}$ in July from the Base (blue line) and MetEmis scenarios (red line).

95
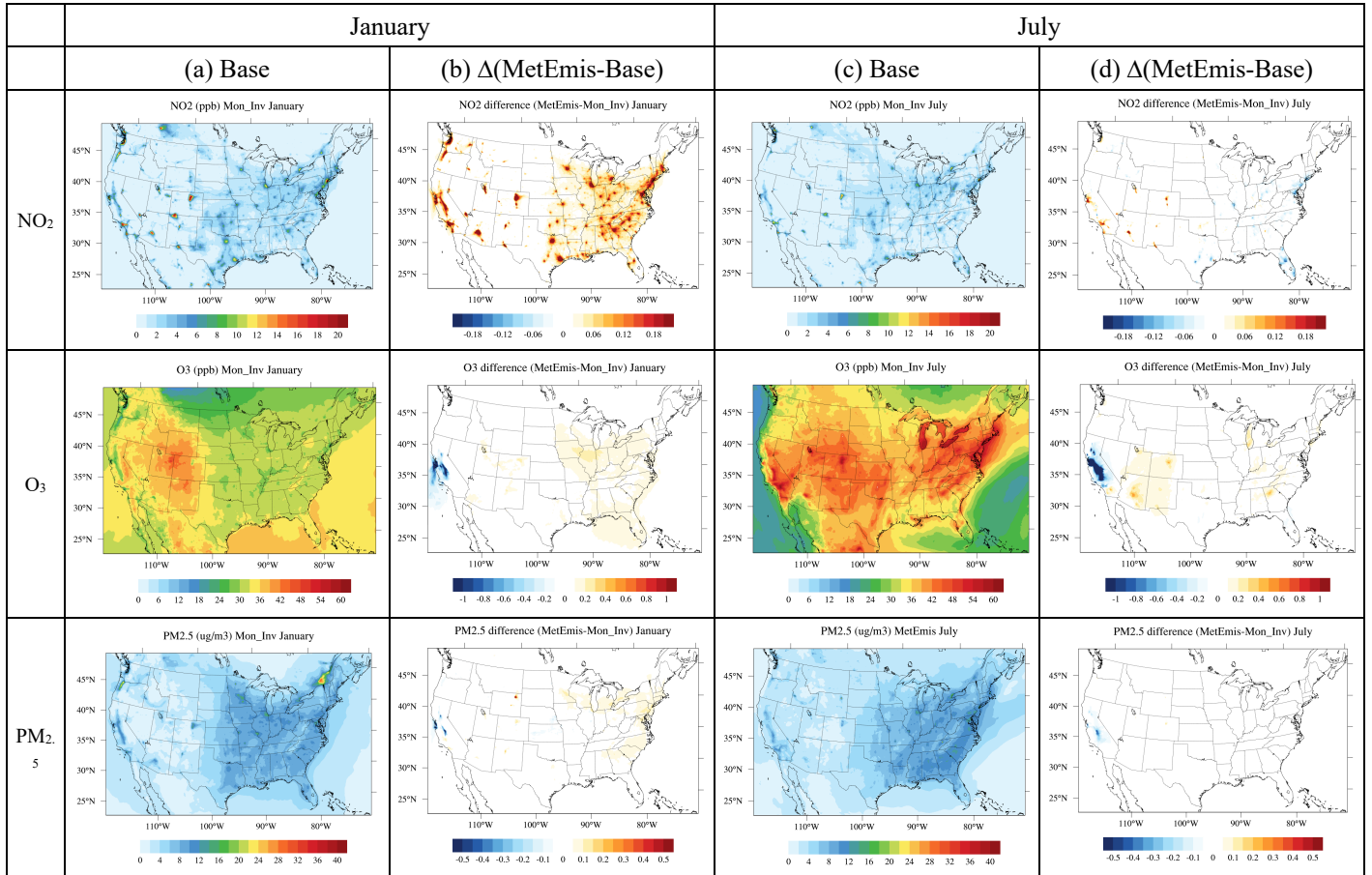
Figure 5. spatial distribution of NO2, O3 and PM2.5 concentrations and difference figures: (a) January averaged concentrations from Base scenario, (b) the differences between Base and MetEmis scenarios in January, (c) July averaged concentrations from Base scenario, and (d) the differences between Base and MetEmis scenarios in July
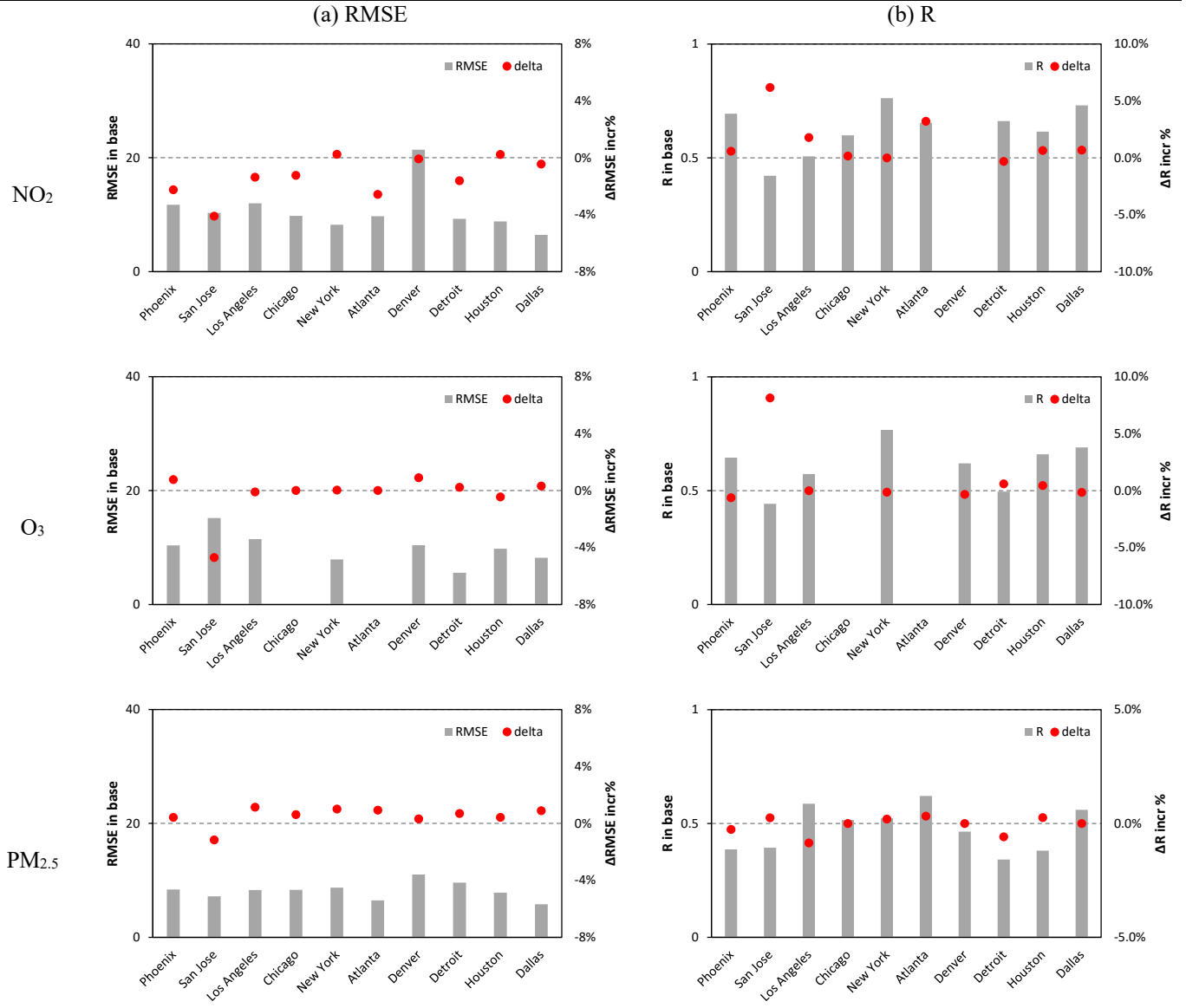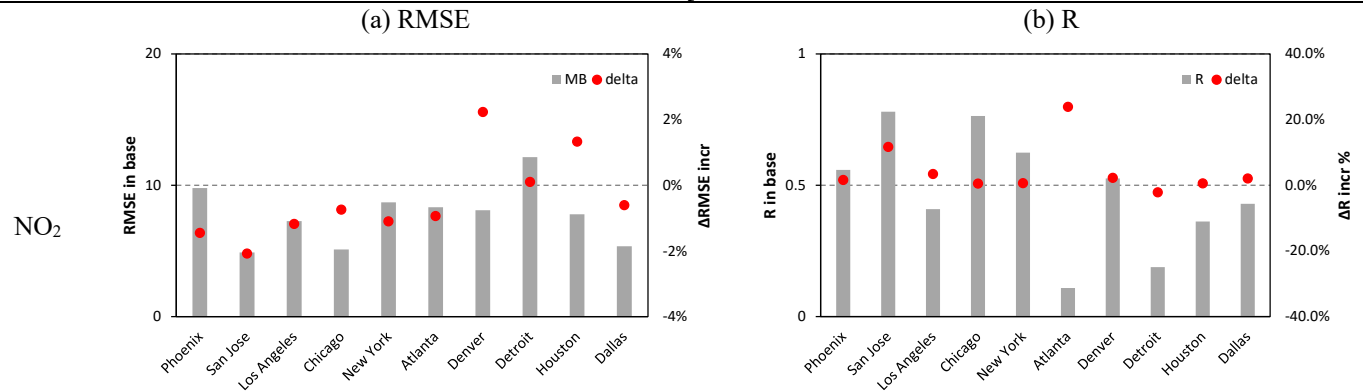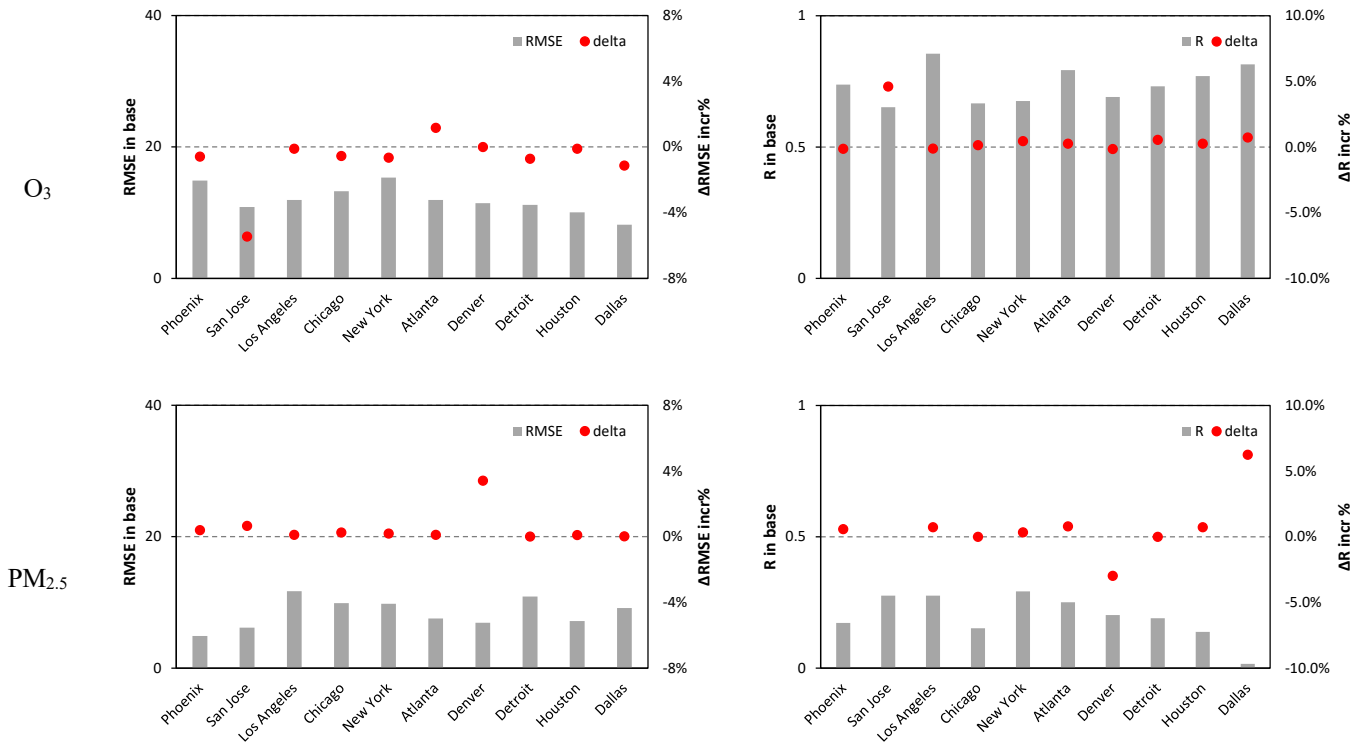
Figure 6. Comparison of model performance in simulating NO$_2$, O$_3$ and PM$_{2.5}$ concentrations between Base and MetEmis scenarios. The columns panels show the different model evaluation metrics in January (panel a and b) and July (panel c and d). The rows present different species including NO$_2$, O$_3$, and PM$_{2.5}$. RMSE is Root-mean-square deviation, R is correlation coefficient. delta is (MetEmis - Base)/Base; when $\Delta R > 0$ and $\Delta RMSE < 0$, indicate the improvement in MetEmis.

* NO$_2$ in January in Denver is -0.002, increased to 0.008 with MetEmis; Observed O$_3$ data is missing in Chicago and Atlanta in January.
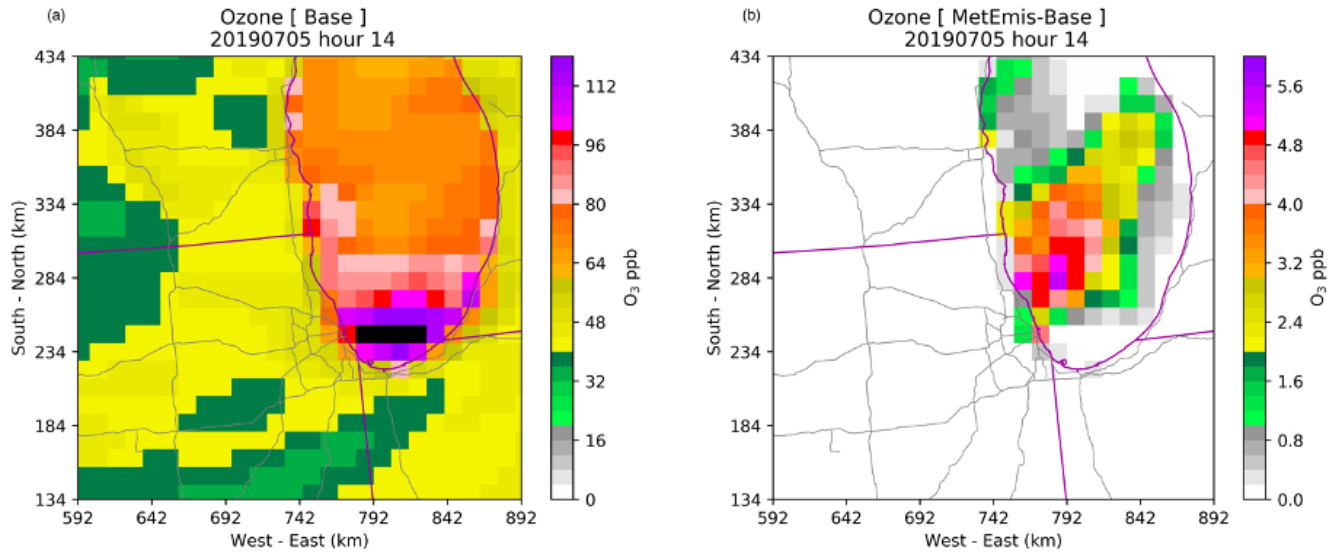
Figure 7. Base hourly ozone (ppb) (a) and the hourly ozone difference (MetEmis-Base) (b) at 14LST on July 5th, 2019. Black color indicates the concentration above the color scale maximum (120 ppb)
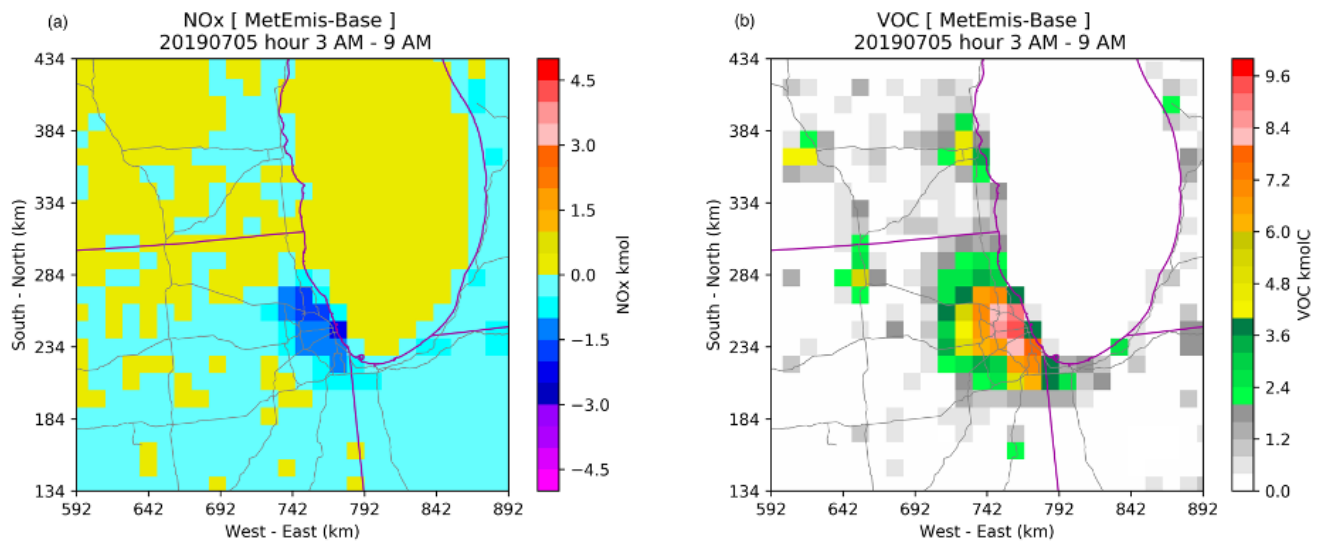
Figure 8. Spatial differences of NOx (a) and VOC (b) emissions in early morning (3AM-9AM) on Jul 5th, 2019.
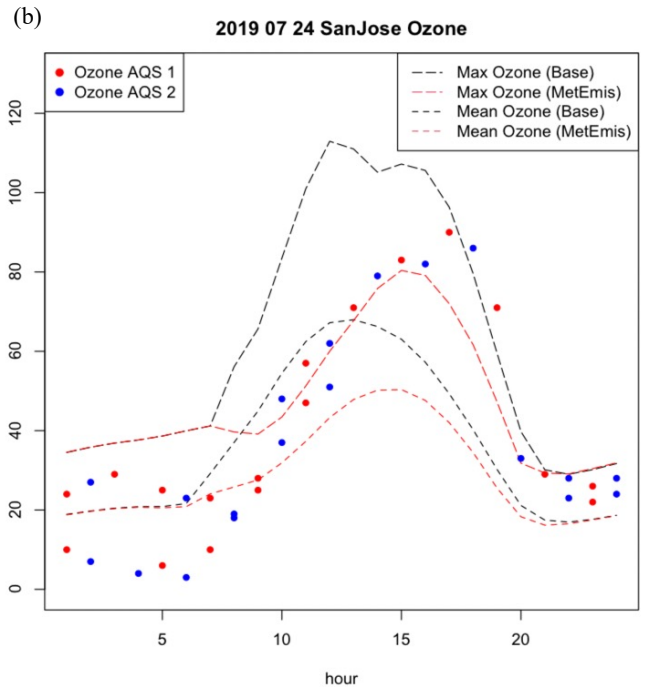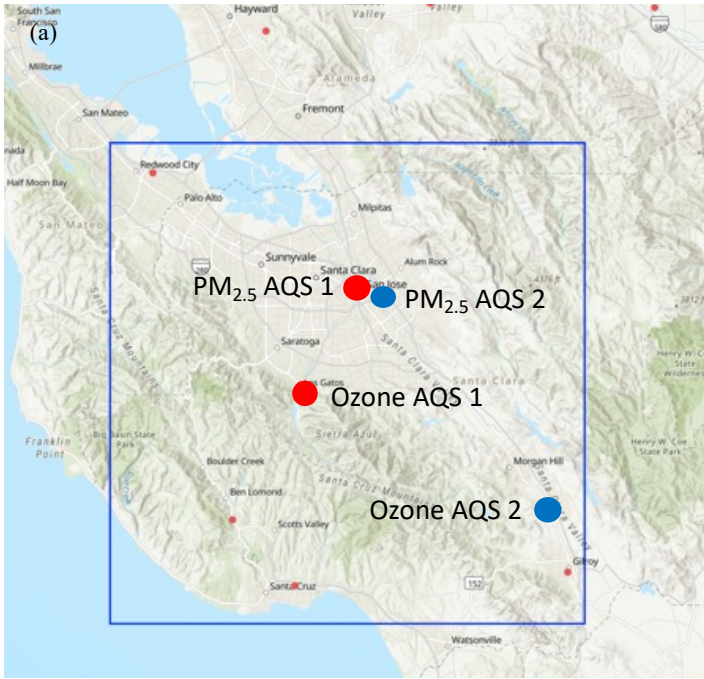
Figure 9. (a) U.S. EPA's Air Quality System (AQS) ozone and PM$_{2.5}$ monitoring locations, and (b) diurnal variation of ozone (maximum and mean) on July 24, 2022 over San Jose, CA. The base map layer of this figure was made by Esri (Esri, 2013).
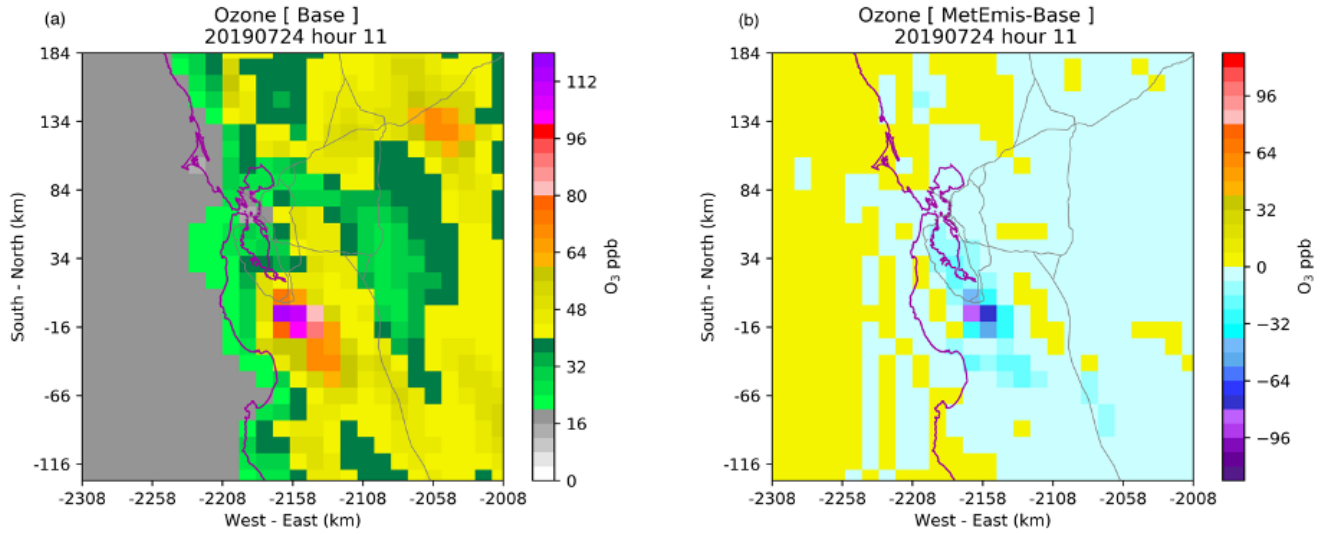
Figure 10. Base hourly ozone concentration (ppb) (a) and the hourly ozone difference (MetEmis-Base) (b) at 11LST on July 24th, 2019.
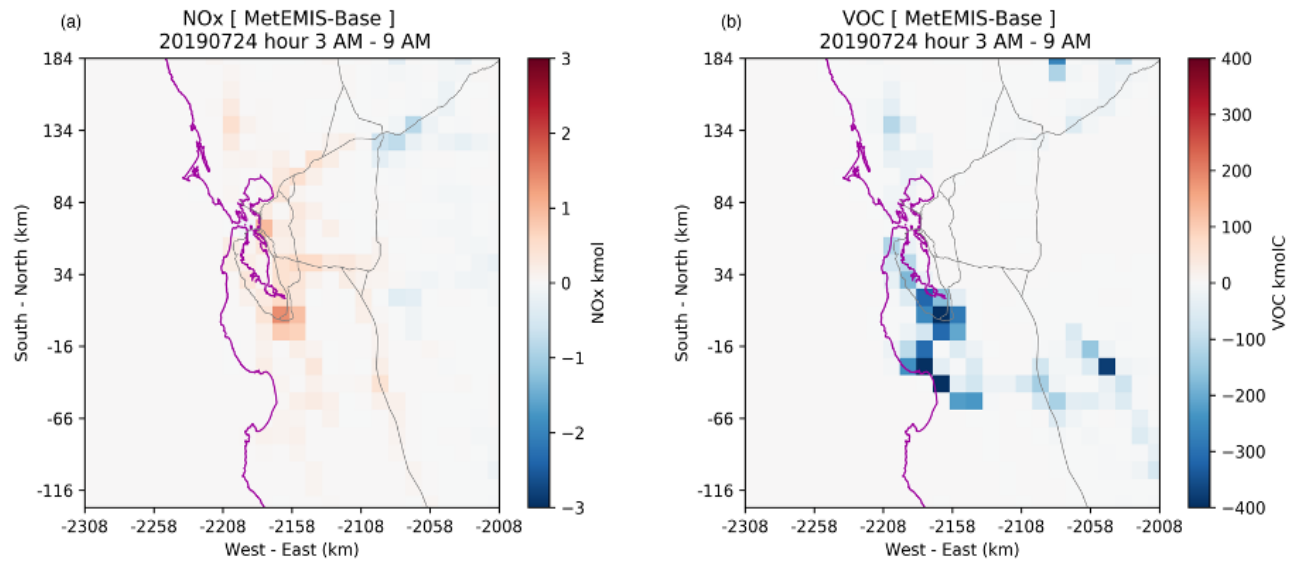
Figure 11. Spatial differences of NOx (a) and VOC (b) emissions from 3LST to 9LST on July 24, 2019 over San Jose, CA.

95
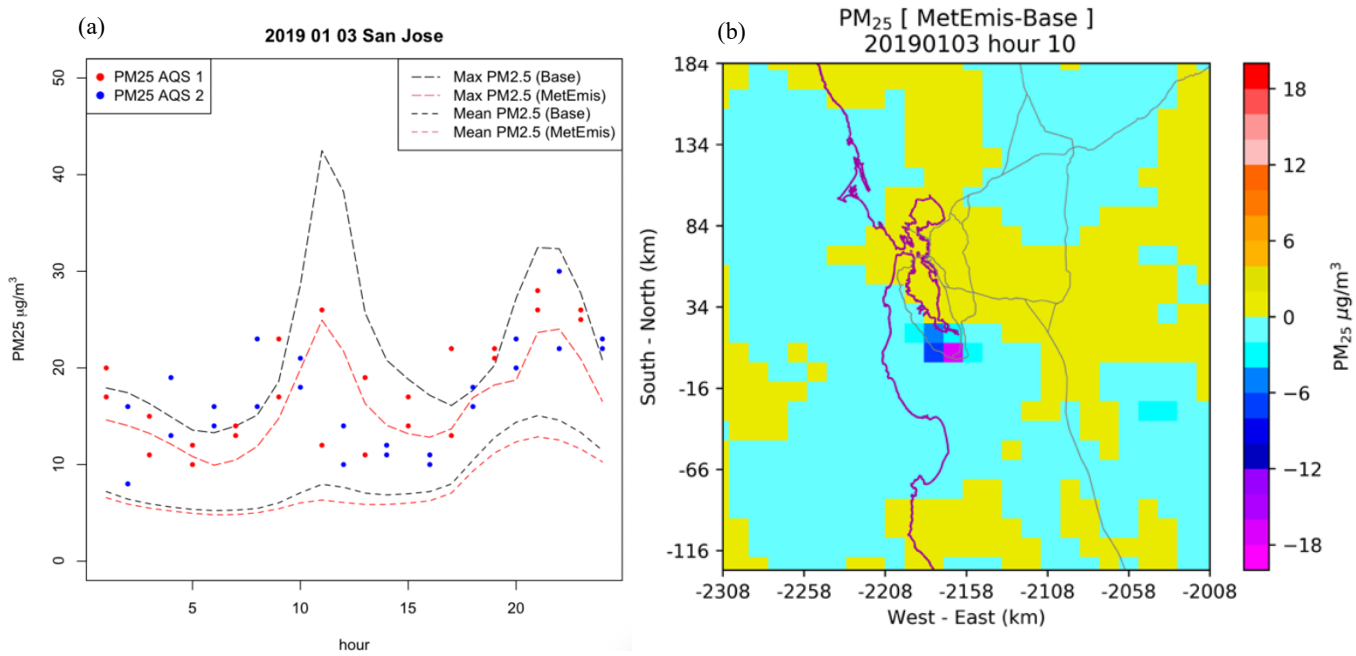
Figure 12. (a)Diurnal variation of PM$_{2.5}$ (maximum and mean) concentrations over San Jose targeted region, and (b) the spatial difference of PM$_{2.5}$ at 10LST on January 3, 2019.
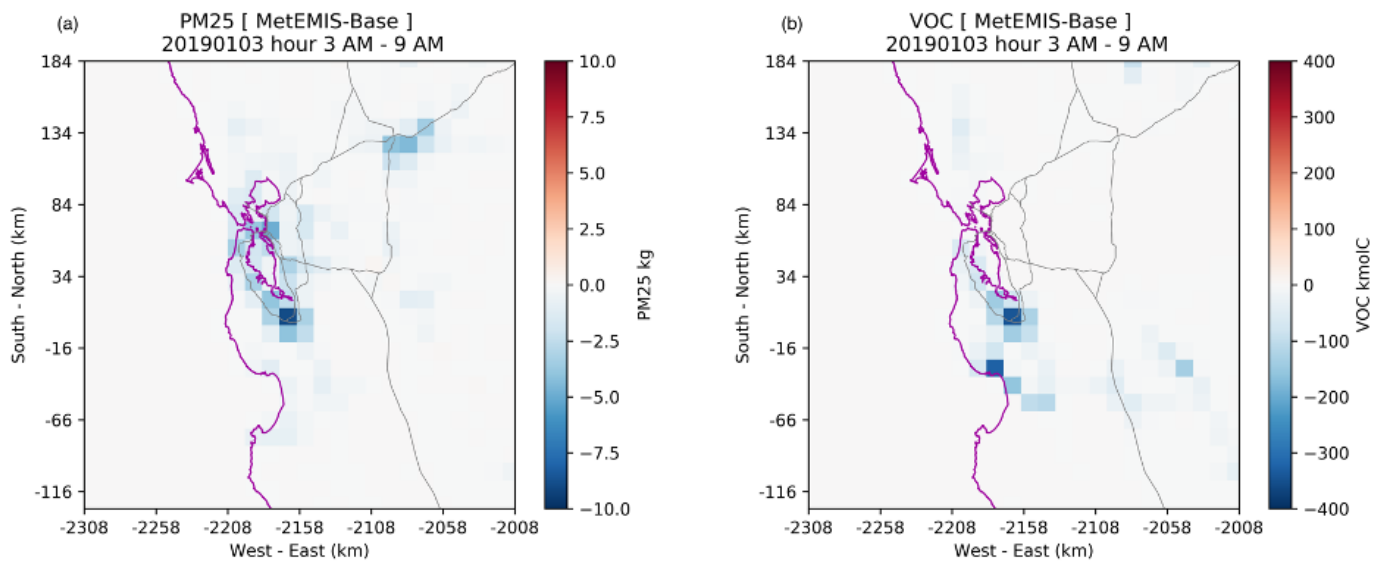
Figure 13. Spatial difference of PM$_{2.5}$ (a) and VOC (b) emissions over San Jose region from 3LST to 9LST on January 3, 2019.